Thin Solid Films, *250* (1994) 56–60

Growth and structure of polycrystalline Cr/Au multilayered thin films

H. Brückl*, J. Vancea, R. Lecheler, G. Reiss* and H. Hoffmann

Institut für Angewandte Physik III, Universität Regensburg, Universitätsstrasse 31, 93053 Regensburg, Germany

(Received January 1, 1994; accepted April 26, 1994)

Abstract

Metallic multilayered thin films have recently been investigated due to their new magnetic and transport properties. The interest here is focussed on the characterization of the interfaces between the layers. The analysis of growth and structure of polycrystalline Cr/Au multilayers is accomplished by two complementary techniques: *in situ* ultrahigh vacuum scanning tunnelling microscopy and *ex situ* transmission electron microscopy. The combination of these powerful methods provides detailed information about structural characteristics such as crystallite size, surface roughness and crystallographic orientation. Moreover, conclusions can be drawn on the atomic arrangement and growth mechanism at the Cr–Au interface. The results are supported by semiempirical and theoretical expectations.

1. Introduction

The physical properties of metallic multilayered thin films are critically determined by the structure of their interfaces. For instance, in magnetic multilayers there seems to exist an optimal interface structure, smooth on the mesoscopic scale (*i.e.* comparable with crystallite sizes) and somewhat roughened on the atomic scale, leading to enhanced giant magnetoresistance effects [1].

Despite the advancing of grazing-incidence X-ray diffraction as a powerful working method for structural investigations of multilayers a quantitative analysis is still difficult and strongly dependent on the applied model [2]. In this work we have combined *in situ* scanning tunnelling microscopy (STM) with complementary transmission electron microscopy (TEM) studies, the latter only after completion of the multilayers. TEM cross-sections inform about layer periodicity, homogeneity and crystallographic orientation. High resolution electron microscopy, however, needs periodic structures like crystal lattices. Thus in TEM cross-section sharp interfaces can only be recognized, if an exact lining up of the sample and electron beam is provided. A quantitative analysis of interface roughness or local imperfections with TEM is therefore difficult or even impossible. Complementarily, STM gives direct information about the surface topography with atomic resolution. From TEM diffraction patterns additional information such as the crystallographic orientation of the layers can be obtained. This can be utilized in understanding the STM surface images.

In this work we discuss the growth and structure of Cr/Au multilayers. In a second paper the electrical transport properties will be treated and related to their multilayer structure [3]. Under ambient conditions the interdiffusion is only very small in Cr/Au systems [4], which are therefore appropriate for the investigations described above. Additionally, general theoretical models concerning the growth mechanism of a b.c.c. metal (Cr) on an f.c.c. metal (Au) are still under discussion. The system studied is polycrystalline. Thus the growth behaviour at grain boundaries and on crystallites is quite complex. Experimental data on this subject are rare, mainly due to this complexity.

2. Experimental details

$(\mathrm{Cr}\ d_{\mathrm{Cr}}/\mathrm{Au}\ d_{\mathrm{Au}})_N$ multilayers (where d denotes layer thickness) were evaporated on Corning Glass 7059 substrates in ultrahigh vacuum (UHV) of 1×10^{-9} mbar or lower. N denotes the number of double layers. The substrates were thermally stabilized to 300 K during the deposition. An Au wire with purity of 99.999% was evaporated from an Al_2O_3 crucible at a deposition rate of 0.5–1 nm min^{-1}. Cr crystallites of electrolytic purity (99.99%) were sublimated from a tungsten basket (rate, 0.3–0.5 nm min^{-1}). The mean film thickness was controlled during evaporation by a quartz monitor, which was calibrated by Tolansky interferometry and quantitative X-ray fluorescence analysis. Thus the uncertainty of the layer thickness was below 5%. The layer thickness ranges were $d_{\mathrm{Cr}} = 0–4$ nm and $d_{\mathrm{Au}} = 4–15$ nm. The preparation procedure could be stopped at any stage of the film growth, and subsequently the surface topogra-

*Present address: Institut für Festkörper- und Werkstofforschung Dresden (IFF), PO Box, 01171 Dresden, Germany.

0040-6090/94/$7.00
SSDI 0040-6090(94)06186-O

phy could be scanned *in situ* by UHV STM. By this way STM images of the main growth stages of the multilayers were obtained.

The home-made UHV scanning tunnelling microscope allowed a vertical resolution better than 0.005 nm. The lateral resolution for mesoscopic structured surfaces, however, was limited by the radius of the very end of the tips (cut Pt wire). An estimation according to Ref. [5] gives radii of about 5 nm leading to a maximum error of 10% for all corrugation heights reported in this paper. Typically, tunnelling current values of 1–10 nA and bias voltage of 10–100 mV were used. TEM investigations were carried out with a Philips CM30.

In the following the structure of the first Cr layer will be sketched. Secondly, the results of Cr/Au double-layered films are presented, which serve as substrates for the multilayers. The structure and growth of further Cr and Au layers are described. Finally, the growth mechanisms of the multilayer system are discussed with regard to the results for the basic double layer.

3. Results

3.1. Cr layers on glass substrates

Cr films on glass exhibit a rather complex growth mechanism in the initial stage. Gasgnier and Nevot [6] proposed the formation of an adherence oxide zone of ~ 1 nm thickness, prior to the polycrystalline film growth. STM imaging became possible at a critical thickness of 2.0 nm, *i.e.* for electrically continuous films. In this early growth stage small Cr agglomerates cover irregularly shaped topographical elevations, which can be assigned to the initial reaction zone. This behaviour can be clearly seen in the STM scan of Fig. 1. With increasing film thickness the agglomerates grow to crystallites with a mean diameter of 15–20 nm. For $d_{Cr} \geq 4$ nm the shapes of the crystallites as well as the surface corrugations remain unchanged. The films are polycrystalline with a mean corrugation height of $\Delta H \approx 1$ nm, which is defined as the half-height full width in STM height amplitude histograms. For the multilayers described here the typical thickness of the first Cr layer amounts to 2.0 nm. Thicker precoatings did not change the main results concerning the structure of the multilayer.

3.2. The first Au layer on Cr

In Fig. 2 an STM image of a typical surface of polycrystalline Cr/Au double layers is shown. The mean size of the flat Au crystallites averaged over several samples ranges from 40 to 60 nm in full agreement with TEM images. They correspond to the values found for Au on glass. The mean grain size is thickness independent in the range $d_{Au} = 3$–100 nm. Accordingly, the surface corrugation of $\Delta H \approx 2$ nm remains constant, too. Compared to Au films on glass ($\Delta H \approx 5$–6 nm) the Cr precoating strikingly reduces the mean corrugation height (but not the grain size).

The adhesive properties of Cr cause a reduced surface mobility of Au atoms. The resulting higher density of condensation nuclei allows a flat film growth. The Au overlayer becomes continuous at a thickness of $d_{Au} = 3$ nm. Accordingly, the small initial clusters must grow to crystallites of the same extension as in the Au/glass system. Indeed STM images of double layers with an Au thickness of $d_{Au} = 2$ nm show island-like features. The reason for this growth mechanism accompanied by the formation of texture (tackled below) is not clear yet. We suggest a coalescence-like recrystallization process, driven by the surface tension of the small Au clusters.

For $d_{Au} \geq 3$ nm the surface topography remains unchanged and looks quite like that depicted in Fig. 2. Au atoms are therefore homogeneously adsorbed on a con-

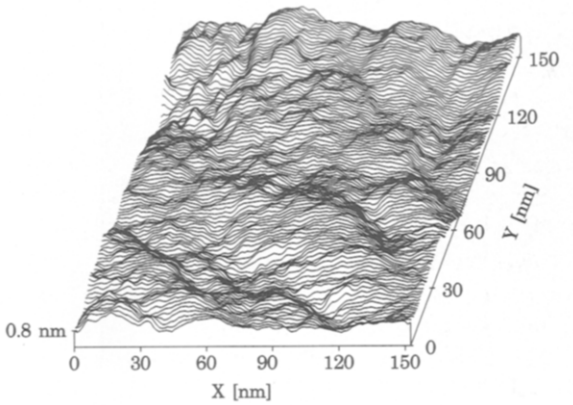

Fig. 1. STM line scan of a Cr film on glass with $d_{Cr} = 2$ nm, deposited at $T_S = 300$ K.

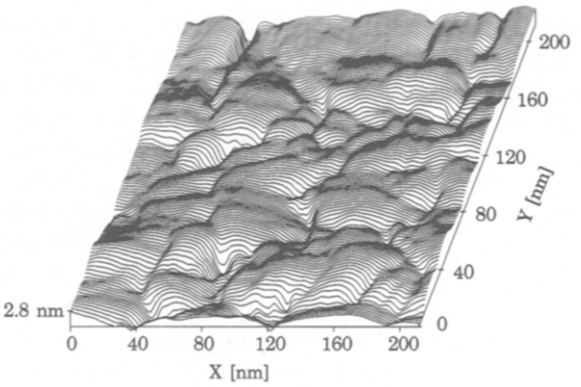

Fig. 2. STM line scan of surface of a (Cr 2 nm/Au 20 nm) double layer ($T_S = 300$ K).

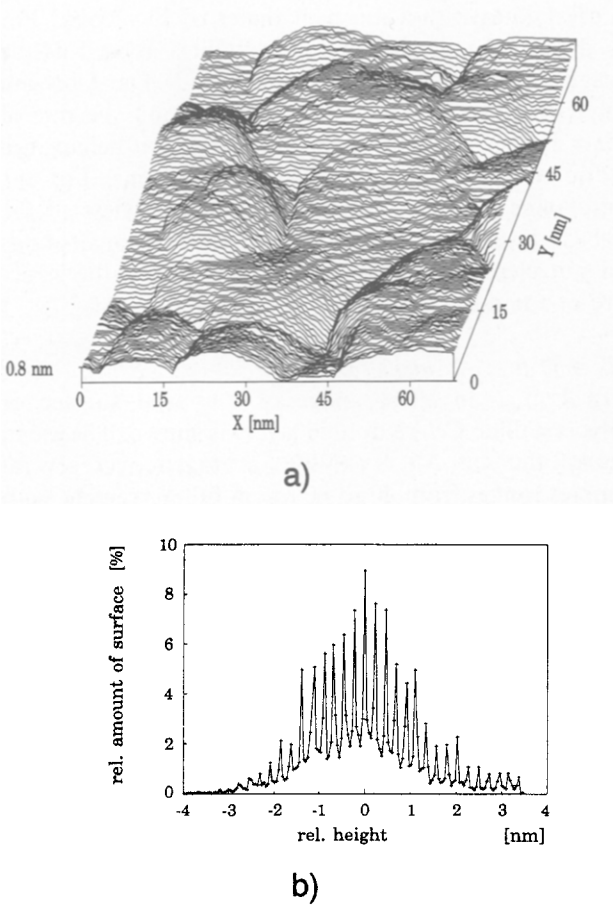

Fig. 3. (a) High resolution STM line scan of the surface of a (Cr 1.5 nm/Au 20 nm) double layer. (b) Corresponding height amplitude histogram of the image (a).

tinuous Au cover film leding to an invariant surface topography by increasing film thickness.

The microstructure of the surface can be observed on an atomic scale in Fig. 3(a). The crystallites consist of flat terraces separated by atomic steps. The step height can be evaluated from the height histogram of Fig. 3(b): the mean value of 0.235 ± 0.015 nm can be assigned to the interplanar spacing of f.c.c. Au in the [111] direction. As only (111) steps are found, a strong texture can be derived, which is clearly confirmed by TEM microdiffraction at single Au crystallites (Fig. 4). The individual crystallites exhibit the preferential [111] direction normal to the film plane, but are randomly arranged in the film plane. The mean lateral extension of the terraces was estimated at $\xi \approx 1$ nm using the correlation length of the radial autocorrelation function taken from the STM image of Fig. 3(a). This small value results mainly from the numerous narrow terraces near grain boundaries, which overcome the extended terraces of width up to 10 nm on the top of the crystallites. In contrast to this, the Au films on glass (i.e. without Cr precoating) exhibit a much smaller degree of (111) texture.

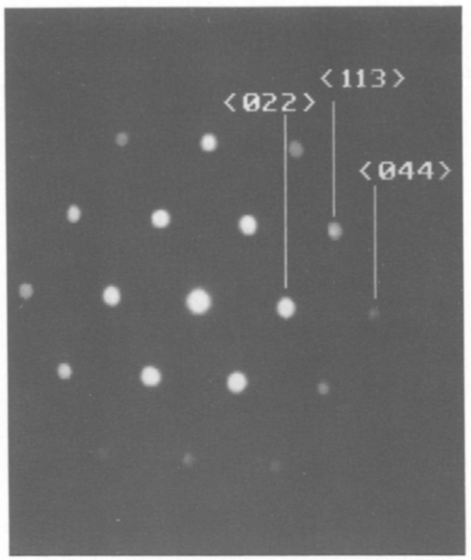

Fig. 4. TEM microdiffraction at an individual Au crystallite of a (Cr 1.5 nm/Au 10 nm) double layer (inclination of the electron beam to the film plane, 90°). Indices are crystallographic directions.

3.3. The characterization of the multilayers

3.3.1. STM investigations

In order to obtain multilayers the Cr/Au double layers discussed above are first covered with a thin second Cr layer. The STM image in Fig. 5 represents the typical surface topography of a second Cr layer 2 nm thick. The contours of the buried Au crystallites can still be recognized. Smaller Cr crystallites have been grown on the top. These are regularly shaped and mostly elongated along the terrace steps of the underlying Au(111) surface. The average extension of the Cr

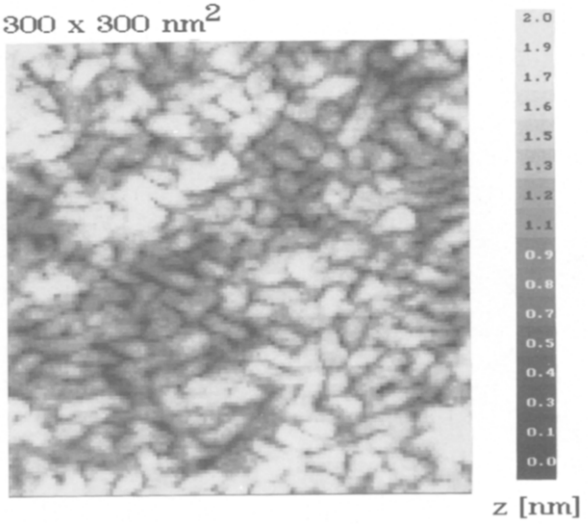

Fig. 5. Grey-scale STM image of a (Cr 2.0 nm/Au 10 nm) double layer covered by 2.0 nm of Cr.

crystallites amounts to about 15 nm. Thus each Au crystallite is covered by about ten Cr hillocks.

The frequent appearance of 60° and 120° angles between the elongated Cr crystallites gives rise to the assumption that a preferential growth exists along the closest packed atom rows on the (111) surface, *i.e.* the terrace steps. Highly resolved STM images of about one-half of a Cr monolayer give no support to an accumulation of Cr atoms at the terraces themselves. The first arriving Cr adatoms grow therefore in a two-dimensional manner. A direct localization of the Cr adsorption sites was not possible, because the material contrast was too faint when running STM in spectroscopic mode. The STM images of the subsequent three-dimensional growth illustrate that the Au terrace steps did not act as fundamental barriers for the Cr adatoms: the Cr hillocks are observed to extend over several terraces.

The anisotropic growth of the Cr crystallites continues down to the grain boundary valleys leading to a filling of the grooves accompanied by an overall smoothing of the surface. The overall mean roughness ΔH is considerably reduced in this way. The observed local mean roughness of $\Delta H_{loc} = 1$ nm is mainly caused by the Cr crystallites themselves.

The oriented growth of Cr along Au(111) terrace steps can be qualitatively understood by the Nishiyama–Wassermann (NW) growth mechanism [7] for the Au(111)/Cr(110) system. The lattice misfit along the $\langle 1\bar{1}0 \rangle$ atom rows is very small (less than 0.02%). This $\langle 1\bar{1}0 \rangle$ direction runs along the edges of the Au(111) terrace steps. Vertically there is no lattice matching. Consequently the anisotropic growth behaviour is favourable. The transition from the initial smooth growth to three-dimensional anisotropically shaped crystallites is a result of the interaction between adhesion and surface energy.

Similar growth was found for b.c.c. Fe(110)/f.c.c. Au(111) by Marliere *et al.* [8]. By combined reflection high energy electron diffraction, small-angle X-ray reflection and TEM analysis they showed that several smaller Fe crystallites twisted by 120° angles relative to each other grow on each one of the Au(111) crystallites.

The essential topographic feature of the following second Au layer is the smoothing out of the small-scale hilly 'landscape' of the second Cr layer and the restoring of Au grain boundaries on a larger scale. Typical STM scans for these surfaces resemble that of the first double layer (see Fig. 2). Flat Au crystallites ($\Delta H \approx 1.7$ nm) again laterally extend to mean sizes of $D = 40$–60 nm. The large grains of Au on Cr may be induced by the high mobility of Au on Au [9], when a compact cover layer was already formed. Additionally, the smaller surface energy of Au ($\gamma_{Au} = 1.626$ J m^{-2}) leads to larger grains than in the case of Cr ($\gamma_{Cr} = 2.056$ J m^{-2}).

The growth behaviour of the second double layer discussed above repeats for each additional Cr/Au layer. The multilayer is growing by adding identically structured double layers. Even for $N > 7$ only (111) steps have been found in highly resolved STM images of the topmost Au layer suggesting a continued textured growth through the stacked layers. The ordered Cr interlayers must transfer this texture from the preceding Au layer to the next one.

The unchanged intermittent structural characteristics (step height, crystallite size, ordered anisotropic growth) of the multilayers suggest the existence of a layered superlattice within the (111) textured crystallites. The requirements reported by Bauer and van der Merwe [10] seem to be fulfilled, as follows.

(a) In a layered superlattice only NW-type growth should occur. A mixing of different growth modes is prohibited for oriented growth. For the Cr/Au system the misfit factors ρ are close to the stability criteria for NW-type growth: $\rho_{CrAu} = 0.868$ and $\rho_{AuCr} = 1.155$ [7].

(b) The compatibility factor ($\Gamma_{AuCr} = 0.234$) measuring the misfit of the surface energies of the two components is smaller than the empirical critical values of 0.5.

3.3.2. *Complementary TEM investigations*

The TEM cross-section image given in Fig. 6 shows a well-resolved layer structure. Grain boundaries propagate vertically through the whole multilayer. The STM result of the invariance of the crystallite size in each Au layer is thereby clearly confirmed. A quantitative interpretation of the distorted zones and defects in Fig. 6, however, is problematic. A clear statement concerning the interface construction or roughness of the individual layers is difficult due to the smeared contrast at the interfaces. It is therefore impossible to extract the

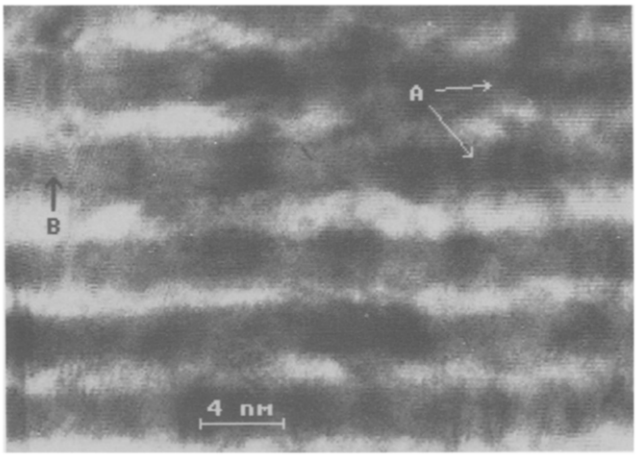

Fig. 6. TEM cross-section of a (Cr 1.5 nm/Au 2.5 nm)$_7$ multilayer. A denotes lattice lines in Au layers, B denotes distorted zones at grain boundaries.

growth mechanism of these multilayers from TEM images only. STM, however, can provide complementary information including roughness and local atomic arrangement at the interfaces.

Additionally, TEM microdiffraction patterns for the cross-sectioned multilayers have been analysed. These patterns were taken from individual column regions marked by the vertical grain boundaries propagating through seven or more double layers. They looked like diffraction patterns of single Au crystallites. Consequently, a textured, respectively ordered, growth through the whole column region should be present. For inclined electron beam exposition the slightly sickle-like spots indicate that only a small azimuthal torsion of the parallel (111) planes by about 5° exists. The Cr diffraction pattern was not visible due to the low form factor and low thickness.

Moreover, the cross-section in Fig. 6 reveals horizontal Au(111) lattice lines ($d_{(111)} = 0.235$ nm) inside the crystallites. These are well separated by distorted regions, *i.e.* by the grain boundaries. The results presented above can merely be understood by the existence of a layered superlattice through the whole column region. However, we have to keep in mind that this insight has been already suggested by the STM results.

4. Conclusion

The application of *in situ* UHV STM in connection with TEM cross-section images allows a detailed analysis of the multilayer growth and structure. These two methods inherently provide complementary information. TEM as a diffraction instrument works in reciprocal space, and is therefore mainly sensitive to periodic structure, *e.g.* crystal lattices. STM gives information in real space, especially about interface roughness, local atomic arrangement etc. With these two methods we were able to characterize the growth and structure of Cr/Au multilayers reliably.

The first Cr base layer consisting of small crystallites displays a smooth surface mainly due to the existence of an adherence oxide zone on the glass substrate. The Cr precoating causes a smooth growth of the next Au layer with large and flat crystallites. The interface roughness and the crystallite size of the further Au layers spaced by Cr remain unchanged through the whole multilayer. In every double layer the surface of the Au crystallites themselves is made up of (111) terrace steps. Thus the multilayer is constructed of identical Cr/Au double layers. The initial (111) fibre texture of the first Au layer represents the starting stage of an NW-type growth of successive Cr and Au layers, leading to a layered superlattice in each single crystallite at least. Neighbour crystallites are randomly oriented with respect to the in-plane direction.

Acknowledgments

The authors acknowledge the help of M. Mändl and J. Zweck for TEM experiments and valuable discussions. This work was supported by Deutsche Forschungsgesellschaft.

References

1 F. Petroff, A. Barthelemy, A. Hamizic, A. Fert, P. Etienne, S. Lequien and G. Cruezet, *J. Magn. Magn. Mater.*, *93* (1991) 95. M. Jacob, G. Reiss, H. Brückl and H. Hoffmann, *Phys. Rev. B.*, *46* (1991) 11208.
2 M. Piecuch and L. Nevot, in A. Chamberod and J. Hillairet (eds.), *Metallic Multilayers*, Trans Tech, Hedermannsdorf, 1990.
3 H. Brückl, J. Vancea, G. Reiss and H. Hoffmann, in preparation.
4 P. Madakson, *J. Appl. Phys.*, *70* (3) (1991) 1380.
5 G. Reiss, F. Schneider, J. Vancea and H. Hoffmann, *Appl. Phys. Lett.*, *57* (1990) 867.
6 M. Gasgnier and L. Nevot, *Phys. Status Solidi A*, *66* (1981) 525.
7 L. A. Bruce and H. Jaeger, *Philos. Mag. A*, *38* (2) (1978) 223.
8 C. Marliere, J. P. Chauvineau and R. Renard, *Thin Solid Films*, *189* (1990) 359.
9 C. A. Lang, M. M. Dovek, J. Nogami and C. F. Quate, *Surf. Sci.*, *224* (1989) L947.
10 E. Bauer and J. H. van der Merwe, *Phys. Rev. B.*, *33* (6) (1986) 3657.